HEAT AFTER DEATH

S. Pons
M. Fleischmann
IMRA Europe, S.A.
Science Centre
220, Rue Albert Caquot
Sophia Antipolis, 06560
FRANCE

Abstract

We have described elsewhere (e.g. see [1,2]) that Pd and Pd–alloy electrodes cathodically polarised in D_2O solutions under extreme conditions can drive the calorimetric cells to the boiling point. We have then adopted the procedure of allowing the cells to boil to dryness. For these conditions the galvanostats are driven to the rail voltage (100 V) but the cell current is reduced to zero. We have then found that cells which contained D_2O frequently remain at high temperatures (in the vicinity of 100°C) before cooling rapidly to the bath temperature. Cells containing H_2O can also be driven to the boiling point but such cells cool immediately on terminating the experiments.

This phenomenon has become known as "Heat after Death" (the death referring to cessation of polarisation). Calibrations of the cells for such conditions show the generation of high levels of enthalpy at zero enthalpy input.

Methods of investigating such systems will be outlined.

Introduction

We have recently reported that Pd or Pd–alloy cathodes polarised in 0.1M LiOD in D_2O can be driven to give high rates of generation of the specific excess enthalpy provided the cell temperature is allowed to rise progressively with time[1,2] (see also [3]; for an explanation of the required experimental protocol see [4]). These intense rates of heating (up to $\sim$ 4kW cm^{-3}) lead to the "boiling to dryness" of the electrolyte in the "open cells" used in these experiments* and it was noted that such extreme conditions may be followed by prolonged periods (several hours) during which the cells remain at high temperatures at zero or very low levels of power input, a phenomenon which has become known as "Heat after Death" (for reports of related phenomena see[6,7]; our first observations of these effects using these particular cells and protocols were made in May/June 1990 although a number of earlier observations are also most easily explained as having been caused by "Heat after Death").

In a reply[5] to a critique[8] of these publications[1,2] we pointed out that we had refrained

*The Dewar-type calorimetric cells, see Fig 5[4], have rates of increase of the heat transfer with temperature of the order 0.1W K^{-1} and temperatures in the region of the boiling point are reached at total rates of enthalpy input $\sim$9W. Such conditions are achieved for Pd-based cathodes at current densities in the range 0.5–0.7 A cm^{-2} (typical cell current 0.5 A). Foaming of the electrolyte or spray formation is negligibly small under these conditions.[5]

from interpreting the "Cooling Curves" which characterise these episodes of "Heat after Death" because we believed that the calorimeters used are not well suited for making exact evaluations under such conditions. In the present paper we outline a number of possible approaches to the analysis of these "Cooling Curves." The results obtained show that our initial assessment of the performance of the calorimeters was too pessimistic: in the absence of excess enthalpy generation thermal balances can be made at the 2–3% level in gas filled cells and these errors can decrease to ~0.5% in the presence of excess enthalpy generation.

Experimental

The experimental methods and protocols used were closely similar to those which we have described in earlier publications[1,2,3,9,10] see also[4]). The single compartment Dewar-type electrochemical cells were maintained in water thermostats (up to 4 cells in each thermostat). The temperature of the thermostats was set equal to that of the room housing the experiments; the temperature of the room was controlled to ±0.5°C using two separate control systems. The thermostats were cooled at a controlled rate using subsidiary cooling systems and heated using Techne Te-8A stirrer/temperature control units. We have found that it is possible to control the temperature of each thermostat to within ±0.003°C locally and ±0.01°C overall by adopting this particular strategy (16 thermostats housed in the single thermostatted room). This level of control is essential in order to achieve accurate analyses of the behaviour of the calorimeters (see further below).

The protocols for carrying out the experiments were also similar to those which we have described previously. The electrodes were first charged galvanostatically at low to intermediate current densities for prolonged periods of time; the current density was then raised and this raising of the current density caused a progressive increase of the temperature of the caloriometers up to the region of the boiling point of the electrolyte. Calibrations of the cells were carried out at stated intervals (every 2 days) throughout these two stages by applying constant currents to resistor chains (high stability metal film resistors maintained in heat transfer oil in glass tubes); the voltages developed across the resistor chains were monitored continuously. The heat transfer coefficients for the cells were derived using the methods of analysis described in a further paper presented at this Conference.[4]

The cells were refilled every two days to make up for losses of D_2O due to electrolysis (and due to evaporation at the higher temperatures). The records of the additions show that the Faradaic efficiencies for the electrolyses are close to 100%. As we have noted previously this fact alone is sufficient to show that the reduction of oxygen at the cathodes is negligibly small (deuterium generated at the cathodes cannot be reoxidised at the oxide coated Pt-anodes; for further evidence for negligible reduction of oxygen at the cathodes see[4]). It is important to note that the rate of excess enthalpy generation is zero or positive over the whole period of operation for cells operated using these particular protocols: there is therefore no mechanism for storing energy which could be released when polarisation is interrupted.

Cell and bath temperatures were measured using high stability thermistors (Thermometrics Ultrastable Thermistors, ~10 kΩ ±0.02% stability per year) which were calibrated against National Bureau of Standards calibrated thermometers. The thermistor assembly is shown in Fig 5 of [4]. Cell temperatures were recorded every 300 s: circuits were maintained open for 290 s then closed and readings were taken during the last 1 s using Keithley 199 DMM Scanner Multiscanner Units interfaced to a Compaq 386s/20 computer.

The only major change to the calorimeters compared to the instruments described in our earlier publications was the addition of a Pt–wire helical resistor to "empty" cells. This was driven galvanostatically with power inputs in the range 0.1 to 9 W. It was found that the cell temperatures reached constant plateau values at long times (constant to within ±0.005°C); with this range of power inputs the range of the plateau temperatures straddled the operating range of the calorimeters, 20°C< θ_{cell} <100°C. Heat transfer coefficients were determined from the plateau values of the temperature using the simple relation

$$k'_R = \frac{\Delta\theta}{[(\theta_{bath} + \Delta\theta)^4 - \theta^4_{bath}]} \tag{1}$$

(all symbols are defined in the glossary of symbols).

Following the interruption of the galvanostatic polarisation of the resistive heater, the cooling curves for such empty cells were determined and compared to the cooling curves for cells showing "Heat after Death" (see below).

Modelling of the Calorimeters

For the simplest conditions of zero energy input during the determination of the Cooling Curves. the general Black Box Model, Fig 6[4]. simplifies to that shown in Fig 1. We note that zero energy input implies zero input to the calibration heaters as well as zero electrolysis current. The latter condition applies with high precision to cells which have boiled dry (see further below) as well as to full cells where electrolysis is interrupted. In turn both conditions imply that there is no input due to make–up with D_2O and no output due to the gas streams. However. it is possible to envisage conditions where evaporation has to be taken into account for cells which are still filled with electrolyte; we will not discuss such cases at this stage.

It follows therefore that we need only consider the time–dependent change of the enthalpy content of the calorimeter and heat transfer to the water bath. The latter is dominated by radiation across the lower, unsilvered portions of the Dewar–type cells. Fig 5[4] (see also [1–3,9,10]). In the absence of any excess enthalpy generation we obtain the simple differential equation

$$C_{P.D_2O,\ell}M^\circ \frac{d\Delta\theta}{dt} = -k'_R[(\theta_{bath} + \Delta\theta)^4 - \theta^4_{bath}] \tag{2}$$

which can be integrated to give the closed form expression

$$ln\left[\frac{y_0(2+y)}{y(2+y_0)}\right] + tan^{-1}(1+y) - tan^{-1}(1+y_0) = \frac{4k'_R\theta^3_{bath}\ t}{C_{P.D_2O,\ell}M^\circ} \tag{3}$$

where

$$y = \frac{\Delta\theta}{\theta_{bath}} \quad . \quad y_0 = \frac{\Delta\theta_0}{\theta_{bath}} \tag{4}$$

In the presence of excess enthalpy generation equation (2) is modified to

$$C_{P,D_2O,\ell}M^\circ \frac{d\Delta\theta}{dt} = Q_f(t) - k'_R[(\theta_{bath} + \Delta\theta)^4 - \theta^4_{bath}] \quad (5)$$

We note that the assumption

$$Q_f(t) = \text{constant} \quad (6)$$

which we have used previously to carry out integrations of the differential equations representing the Black Box Models[1-4,9,10] is unlikely to hold for the phenomenon of "Heat after Death." We are therefore unable to carry out any integration of (5) to give a closed form solution. Two immediate options present themselves for the further analyses of the Cooling Curves:

(i) point-by-point thermal balances based on (5) to give the rates of change of the water equivalent and the rates of radiative cooling, the rates of generation of excess enthalpy being obtained by the difference between these two quantities

(ii) integration of the left-hand and right-hand side of (5):

$$C_{P,D_2O,\ell}M^\circ[\Delta\theta - \Delta\theta_0] = \int_0^t Q_f(\tau)d\tau - k'_R \int_0^t [(\theta_{bath} + \Delta\theta)^4 - \theta^4_{bath}]\, d\tau \quad (7)$$

to give the enthalpy change of the calorimeter, the enthalpy of radiative cooling and, again by difference between these quantities, the excess enthalpy generated in the calorimeter.

Of these two options (i) is subject to the inevitable increase in the errors incurred by the differentiation of the experimental data. The approach (ii) is free from this drawback and is a particular example of the method of data analysis which we now favour for electrodes subjected to cathodic polarisation.[4] It should be noted that the application of both (5) and (6) requires the independent determination of the heavy water equivalent, $C_{P,D_2O,\ell}M^\circ$ and of the heat transfer coefficient. These can be obtained by the methods outlined in a further paper presented at this meeting.[4] In the case of empty cells, a reasonably accurate estimate of $C_{P,D_2O,\ell}M^\circ$ can be obtained by subtracting the contribution of the heavy water content (boiled out during the experiment) from the total water equivalent determined as in [4]. Alternatively, the $\Delta\theta - t$ transients determined during the application of the heating pulse, ΔQ, using the Pt-wire helix can be subjected to a full analysis based on the differential equation analagous to (5)[11]

$$C_{P,D_2O,\ell}M^\circ \frac{d\Delta\theta}{dt} = \Delta Q - k'_R[(\theta_{bath} + \Delta\theta)^4 - \theta^4_{bath}] \quad (8)$$

This analysis gives both $C_{P,D_2O,\ell}M^\circ$ and k'_R; it should be noted that k'_R alone can be obtained from the plateau values of $\Delta\theta$ reached at long times, when $\frac{d\Delta\theta}{dt} = 0$, giving equation (1).

Simple Scenarios for Investigating "Heat after Death"
We observe that there are numerous scenarios for investigating "Heat after Death" using the Cooling Curves determined with calorimeters of the type illustrated by Fig 5.[4] The simplest of these include those listed in Table 1; more complex scenarios include measurements made with partially filled cells. In the present paper we restrict attention to Scenarios 2, 5 and 6 for which we can base the analyses of the Cooling Curves on the approaches outlined in the previous section. We note that the analysis of the cooling Curves for Scenarios 1 and 3 must be based on the full Black Box Model, Fig 6.[4]

Table 1

Simple Scenarios for Investigating "Heat after Death."

1) Cell full:	Cell operated at intermediate temperatures;
	Cell current then reduced in stages.
2) Cell full:	Cell operated at intermediate temperatures;
	Cell current then set to zero.
3) Cell full:	Cell operated at the boiling point:
	Cell current then reduced in stages.
4) Cell full:	Cell operated at the boiling point;
	Cell current then set to zero.
5) Cell empty:	Cell allowed to boil dry;
	Cell then maintained at the rail voltage of the galvanostat.
6) Cell empty:	Cell allowed to boil dry;
	Cell disconnected from the galvanostat.

Results
Scenario 2
4 mm diameter by 12.5 mm length Pd cathode polarised in 0.1M LiOD in D_2O; final cell current: 200 mA: initial temperature for cooling curve: 51.524°C.

We observe first of all that the Cooling Curves for cells following Scenario 2 (cells filled with electrolyte operated at intermediate temperatures with the cell current then set to zero) follow closely the predicted behaviour. equation (3) provided the rate of excess enthalpy generation is close to zero. Fig 2 (see further below). We note that the slope of the plot agrees with that predicted using the independently measured values of $C_{P,D_2O,\ell}M°$ and k'_R. This type of behaviour is also observed for "blank experiments." Pt cathodes in H_2O or D_2O based electrolytes. Pd based cathodes in H_2O based electrolytes. The close fit of the cooling curves to the predicted behaviour shows that k'_R is independent of time, that heat transfer is controlled by the thermal impedance of the vacuum gap of the Dewar type cells and that the temperature within the electrolyte is equilibrated on a time scale short compared to the thermal relaxation time $\frac{C_{P,D_2O,\ell}M°}{4k'_R\theta^3_{bath}}$ of the calorimeters.

We observe next that the presence of any appreciable source of excess enthalpy would cause negative deviations from the straight line plot, Fig 2. The positive deviations at long times would imply a more rapid rate of cooling than that due to heat transfer which is clearly highly unlikely. A more plausible explanation is that the temperature of the thermostat

has been overestimated. That this is in fact likely is shown by the additional plots calculated assuming an error in the temperature readings (±0.005°C). (It should be noted that the maximum variation in temperature throughout the whole space of the thermostat is ±0.01°C; the temperature locally is constant to within ±0.003°C.) These additional plots show that the effects of such errors are negligible provided the interpretation is restricted to values of the ordinate less than 6 and/or times shorter than 45,000 s.

The fact that the excess enthalpy generation is small for this particular experiment following the cessation of the cathodic polarisation is shown by the calculation of the total enthalpy changes according to equation (6), Fig 3. In the results reported in this paper the integrations of the radiative cooling term have been carried out using the trapezium rule except for the blank experiment for Scenarios 5 and 6 where Simpson's rule has been used (see further below). The integral excess enthalpy reaches a value 302 J which is negligibly small compared to the integral of the radiative heat output, 14,191 J (i.e. 2%). It is not clear at the present time whether values of the excess enthalpy of this order of magnitude determined from the cooling curves can be regarded as significant (see further below). In any event we see that the putative rate of excess enthalpy generation (calculated by the point–by–point balance based on equation (5)) drops to very low values within 6 hours following the cessation of polarisation. Fig 4: the thermal balance can be made to better than 0.3 mW at long times. It is of interest that the cell voltage drops rapidly to zero following the cessation of polarisation.

Scenario 4
1 mm diameter by 12.5 mm length Pd cathode polarised in 0.1M LiOD in D_2O; final cell current: 250 mA; initial temperature for the Cooling Curve: 99.605°C.

We examine next the cooling curve for a cell which had been driven into the region of the boiling point but where the polarisation was interrupted before the cell had been allowed to boil dry. Fig 5 gives a plot of the data according to equation (3) and it can be seen that the negative deviations from the predicted line now indicated marked enthalpy generation following the cessation of polarisation. Indeed. there is a period during which the enthalpy generation increases with time as shown by the decrease of the ordinate (although the absolute level of enthalpy generation in this time region is low, see Fig 7 below). The presence of excess enthalpy generation is confirmed by the evaluation of the data according to equaiton (7), Fig 6, and according to equation (5), Fig 7. Fig 6 shows that the integral of the excess enthalpy now reaches 3240 J which is certainly significant compared to the value 302 J for the experiment illustrated in Fig 3. Indeed the value 3240 J equates to 2.9 MJ (Mole Pd)$^{-1}$ which is far beyond the realm of possibility for any chemical process in the system. We also note that for this particular experiment the enthalpy generation initially increases to a very marked peak (0.8 W is about 8 W cm^{-3} for this particular electrode). The further increase in the rate of enthalpy generation at long times accounts for the decrease of the ordinate of the plot according to equation (3), Fig 5.

Scenarios 5 and 6
2 mm diameter by 12.5 mm length Pd cathode polarised in 0.1M LiOD in D_2O; final cell current 500 mA; starting point for Cooling Curve shown on Fig 5.

We turn next to the discussion of one particular phenomenon of "Heat after Death" which was contained in our preceding publications.[1,2] Fig 8 gives the temperature–time data including the period of intense boiling. We note here that the cooling curve was determined initially according to Scenario 5 followed by Scenario 6. For the interpretation of this cooling curve it is important to observe that the cell current fell from the set value

of 500 mA to an indicated value of 0 as the cell boiled dry.† The indication of zero current by the instrumentation of the galvanostat sets an upper bound of 0.5 mA on the measured current and an upper bound of 50 mW on the rate of energy input during the cooling according to Scenario 5 since the rail voltage of the galvanostat used was 100 V (see further below).

In interpreting the behaviour of cells following Scenarios 5 and 6, we must first of all consider the behaviour of appropriate "blank cells." The reason is that the water equivalent of the gas spaces, $\sim$0.1 J K^{-1}, is low compared to that of the solid components of the cells, $\sim$60 J K^{-1}. In consequence, thermal equilibrium may not be maintained at the interface between the gas and the inner wall of the Dewar cell and a significant thermal impedance may appear at this wall in addition to that of the vacuum gap. By contrast the water equivalent of the electrolyte in the filled cells is $\sim$410 J K^{-1} so that thermal equilibrium is readily maintained at the inner wall of the Dewar.

That an additional thermal impedance appears at the inner wall for gas-filled cells is shown by the calibration of these cells using the Pt-wire resistors. The heat transfer coefficients for such gas-filled cells are $\sim$0.6 W K^{-4}, values which are $\sim$0.8 of the values of the cells filled with electrolyte (the latter values are close to those calculated from the Stefan-Boltzmann coefficient and the radiant surface areas). The simplest way of allowing for this additional thermal impedance is to assume that the rate of heat transfer from the gas space to the inner wall is linearly dependent on the temperature difference, $\Delta\Delta\theta$, between those two spaces. If we balance this heat transfer rate, $k\Delta\Delta\theta$, by the radiation across the vacuum gap, then

$$k\Delta\Delta\theta = -k'_R[(\theta_{bath} + \Delta\theta)^4 - \theta^4_{bath}] \tag{9}$$

At a first level of approximation, we can linearise the right-hand-side of (9) giving

$$k\Delta\Delta\theta \simeq 4k'_R\theta^3_{bath}(\Delta\theta - \Delta\Delta\theta) \tag{10}$$

and

$$\Delta\Delta\theta \simeq \left(\frac{4k'_R\theta^3_{bath}}{4k'_R\theta^3_{bath} + k}\right)\Delta\theta \tag{11}$$

and the effective heat transfer coefficient becomes $\left(\frac{4k'_R\theta^3_{bath}}{4k'_R\theta^3_{bath} + k}\right)$. We conclude that although $k > 4k'_R\theta^3_{bath}$ (roughly $k = 16k'_R\theta^3_{bath}$) the magnitude of k is not sufficient to maintain thermal equilibrium at the inner wall of the Dewar.

It is therefore necessary to examine the effect of this additional thermal impedance on the

†Nevertheless we assumed[1,2] that the cell current was maintained at the set value up to the time at which it reached zero. It follows that we overestimated the enthalpy input during the period of intense boiling and that, in consequence, our estimates of the rates of excess enthalpy generation were lower bounds.

shapes of the predicted cooling curves. It is convenient to define

$$\alpha = \frac{k}{4k'_R\theta^3_{bath} + k} \tag{12}$$

and the differential equation (2) then becomes

$$C_{P,D_2O,\ell}M^\circ \frac{d\Delta\theta}{dt} = -k'_R[(\theta_{bath} + \alpha\Delta\theta)^4 - \theta^4_{bath}] \tag{13}$$

We can rewrite (13) in the form

$$C_{P,D_2O,\ell}M^\circ \frac{d(\alpha\Delta\theta)}{dt} = -\alpha k'_R[(\theta_{bath} + \alpha\Delta\theta)^4 - \theta^4_{bath}] \tag{14}$$

giving the solution

$$ln\left[\frac{\alpha y_0(2+\alpha y)}{\alpha y(2+\alpha y_0)}\right] + tan^{-1}(1+\alpha y) - tan^{-1}(1+\alpha y_0) = -\left[\frac{4k\ k'_R\theta^3_{bath}}{(4k'_R\theta^3_{bath} + k)C_{P,D_2O,\ell}M^\circ}\right] t \tag{15}$$

It follows that the form of the solution (3) is unchanged except that y is replaced by αy, y_0 by αy_0 and that the slope of the plot is determined by the effective heat transfer coefficient. In view of the magnitude of α, the effect of the retardation of heat transfer at the inner wall on the shape of the cooling curve is negligibly small.

Fig 9 shows a cooling curve for such a "blank cell" and it can be seen that the cooling curve follows the predicted form (15) down to ~24°C. The fact that deviations are observed below this temperature shows that heat transfer from the gas to the surface of the inner wall of the Dewar must have a more complex dependence on $\Delta\Delta\theta$ than the simple linear relation (8), a result which would indeed be expected.

It is necessary therefore to assess the effect of the deviations from equation (15) on the thermal balances within the cell and, especially, on the magnitude of any excess enthalpy term. Fig 10 shows the relevant terms calculated according to (7). The most important is the integral of the apparent rate of enthalpy production which can be seen to lie between +80 and -80 J although this decreases to -46 J at long times. Fig 10 shows that the variation of $\int_0^t Q_t d\tau$ is systematic rather than random which indicates that this term arises from systematic deviations of the rate of cooling from that predicted by the simple model, equation (15). In any event, the effect of these small enthalpy terms is entirely negligible in comparison with those for cells showing pronounced "Heat after Death" such as that illustrated by Figs 11-13.

Although it is possible to correct for the apparent fall of the heat transfer coefficient with temperature (over the range $0 < \Delta\theta < 5$°C) by using the independently measured values of k'_R, the effect of this fall on the derived excess enthalpies, Fig 10, is negligible compared to the measured values for cells showing high levels of "Heat after Death." We have therefore used the simple formulation developed in this paper for the present stage of the analysis of the Cooling Curves. Fig 11 shows the plot according to equation (3) for such a cell [1,2] and

the marked difference to the behaviour of the "blank cell," Fig 9, will be immediately apparent. The cell remains at high temperature for ~3 hours and the $\Delta\theta$– t plot then indicates a period of cooling roughly in line with that predicted by equation (3). However, this phase of cooling is arrested because a new, lower, level of excess enthalpy generation is reached and the ordinate then again decreases because there is a reheating of the cell contents as for the example discussed above (see Fig 14 below). This lower level of excess enthalpy generation is maintained for a further ~6 hours during which the rate of excess enthalpy generation shows several "spikes," Fig 14. There is then a further period of cooling in line with the predictions of equation (3); we can analyse this region separately by setting the origin at $\Delta\theta$ = 22.408°C, t = 33,337 s, Fig 12. As the curvature of the plot at long times far exceeds that for "blank cells" (e.g. see Fig 7) it is likely that the cell again reaches a new, even lower, level of excess enthalpy generation.

We can again derive the change in the enthalpy content of the calorimeter and the total excess enthalpy by carrying out the integrations as in equation (7). Fig 13 shows that the total excess enthalpy exceeds the total change in enthalpy content of the calorimeter by a factor of nearly 20. An alternative way of displaying this information is to evaluate rates of cooling and the rates of generation of excess enthalpy as in Fig 14. The information derived from this plot has been referred to above.

Discussion

The Cooling Curves which we have observed for cells containing Pd or Pd–alloy cathodes and operated using Scenarios 2, 5 and 6 fall roughly between the limits of the two relevant cases which we have discussed here. At one extreme we have zero or very low levels of enthalpy generation, at the other prolonged and low to high levels of this enthalpy generation: each particular example shows its own particular pattern of behaviour e.g. see Figs 5–7.

Contrary to the view which we have expressed previously, the calorimeters and methodology which we have developed for the investigation of polarised cells also appears to be adequate for deriving a near quantitative interpretation of the Cooling Curves. The systems showing high, sustained, levels of the rates of excess enthalpy generation are naturally of greatest interest because they point the way towards developing systems showing enthalpy generation at low or zero rates of energy input. We note here once again that the excess enthalpy generated in examples such as that illustrated in Fig 13 viz 128.5 kJ (which equates to 3.27 MJ cm^{-3} or 29 MJ $(mole\ Pd)^{-1}$) exceeds by a factor of 10^2 - 10^3 that of any conceivable chemical process. Thus the combustion of all the deuterium stored in the lattice would only generate 148.6 $kJ(mole\ Pd)^{-1}$ assuming that the D/Pd ratio had reached 1. Furthermore, for that particular example, the cell showed excess enthalpy generation throughout the period of polarisation[1,2] so that there was no conceivable mechanism for developing a storage mechanism for chemical or physical energy.

We note finally that cells which show pronounced "Heat after Death" also maintain high cell voltages e.g. see Fig 12. As the Pt counter electrode will rapidly adopt a potential in the vicinity of that of the deuterium electrode, this negative potential must be established at the Pd electrode in contact with the residual solid electrolyte deposited during the phase of "boiling to dryness." It is possible that this highly negative potential is due to the generation of a high surface potential[4,12] which serves to confine the deuterons in the lattice.

Glossary of Symbols Used

$C_{P,D_2O,\ell}$	is the heat capacity of liquid D_2O.	$[JK^{-1}\ \mathrm{mol}^{-1}]$
(k'_R)	is the effective heat transfer coefficient due to radiation.	$[WK^{-4}]$
ℓ	is the symbol for the liquid phase.	
M^0	is the heavy water equivalent of the calorimeter at a chosen time origin.	[mols]
Q_f	is the rate of generation of excess enthalpy.	[W]
$Q_f(t)$	is the time dependent rate of generation of excess enthalpy.	[W]
t	is the time.	$[s]$
v	is the symbol for the vapour phase.	
ΔQ	is the rate of heat dissipation of calibration heater.	$[W]$
$\Delta\theta$	is the difference in cell and bath temperature.	$[K]$
θ_{bath}	is the bath temperature.	$[K]$
τ	is a time.	[s]

References

1. Martin Fleischmann and Stanley Pons in: *Frontiers of Cold Fusion: Proceedings of the Third International Conference on Cold Fusion*, Nagoya, Japan (21-25 October 1992), ed. H. Ikegami, Frontiers Science Series No. 4 (FSS-4) p.47.

2. Martin Fleischmann and Stanley Pons. "Calorimetry of the Pd–D_2O system: from simplicity via complications to simplicity." Physics Letters A 176 (1993) 118.

3. Stanley Pons and Martin Fleischmann in T. Bressani, E. Del Guidice and G. Preparata (Eds), *The Science of Cold Fusion: Proceedings of the II Annual Conference on Cold Fusion*, Como, Italy, (29 June-4 July 1991), Vol. 33 of the Conference Proceedings, The Italian Physical Society, Bologna, (1992) 349, ISBN 887794-045-X.

4. M. Fleischmann, S. Pons, T. Roulette and Monique Le Roux, "Calorimetry of the Pd–D_2O System: the Search for Simplicity and Accuracy." Paper C1.1, presented at the 4th International Conference on Cold Fusion, Maui, Hawaii (December 6-9 1993).

5. M. Fleischmann and S. Pons, "Reply to the Critique by Douglas O.R. Morrison entitled "Comments on Claims of Excess Enthalpy by Fleischmann and Pons using Simple Cells made to Boil" to be published in Physics Letters A.

6. M.C.H. McKubre, B. Bush, S. Crouch-Baker, A. Hauser, N. Jevtic, T. Passell, S. Smedley, F. Tanzella, M. Williams and S. Wing. "Calorimetry Studies of the D/Pd System." Paper No. C1.5, presented at the 4th International Conference on Cold Fusion, Maui, Hawaii (December 6-9 1993).

7. M.E. Mellich and W.N. Hansen, "Pd/D Calorimetry–The Key to the F/P Effect and a Challenge to Science," Paper No. C3.3 presented at the 4th International Conference on Cold Fusion, Maui, Hawaii (December 6-9 1993).

8. Douglas R.O. Morrison, "Comments on Claims of Excess Enthalpy by Fleischmann and Pons using Simple Cells made to Boil." to be published in Physics Letters A.

9. M. Fleischmann, S. Pons, M.W. Anderson, L.J. Li and M. Hawkins, "Calorimetry of the palladium–deuterium–heavy water system." J. Electroanal. Chem., 287 (1990) 293.

10. M. Fleischmann and S. Pons, "Some Comments on the paper Analysis of Experiments on Calorimetry of LiOD/D_2O Electrochemical Cells, R.H. Wilson et al., J. Electroanal. Chem., 332 (1992) 1." J. Electroanal. Chem., 332 (1992) 33.

11. To be published.

12. G. Preparata "Cold Fusion '93: Some Theoretical Ideas." paper No. T1.2 presented at the 4th International Conference on Cold Fusion, Maui, Hawaii (December 6-9 1993).

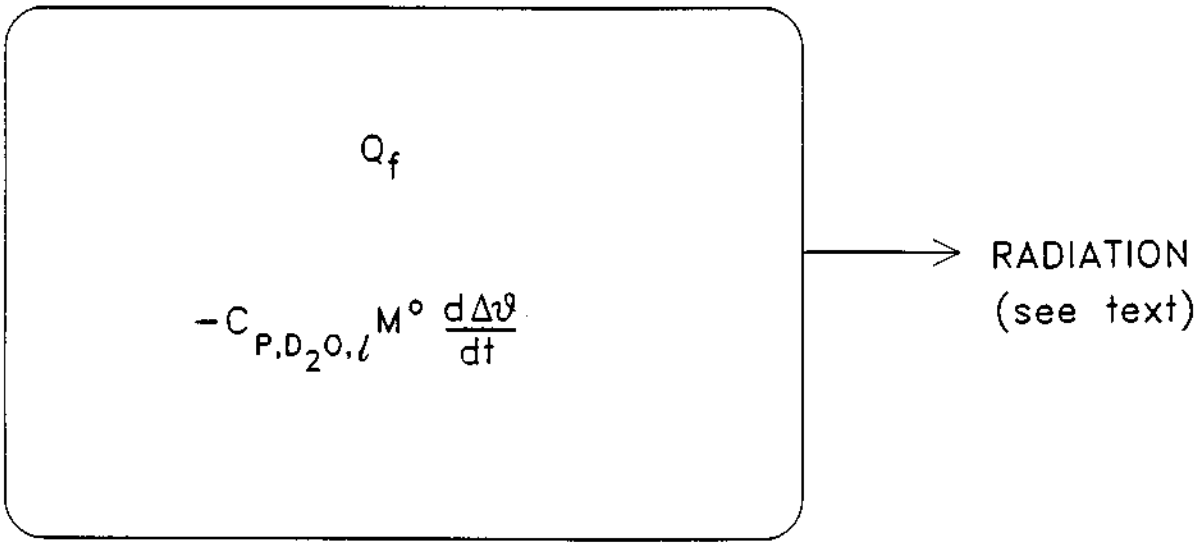

Fig 1. The "Black Box Model" of the calorimeter for the interpretation of cooling curves.

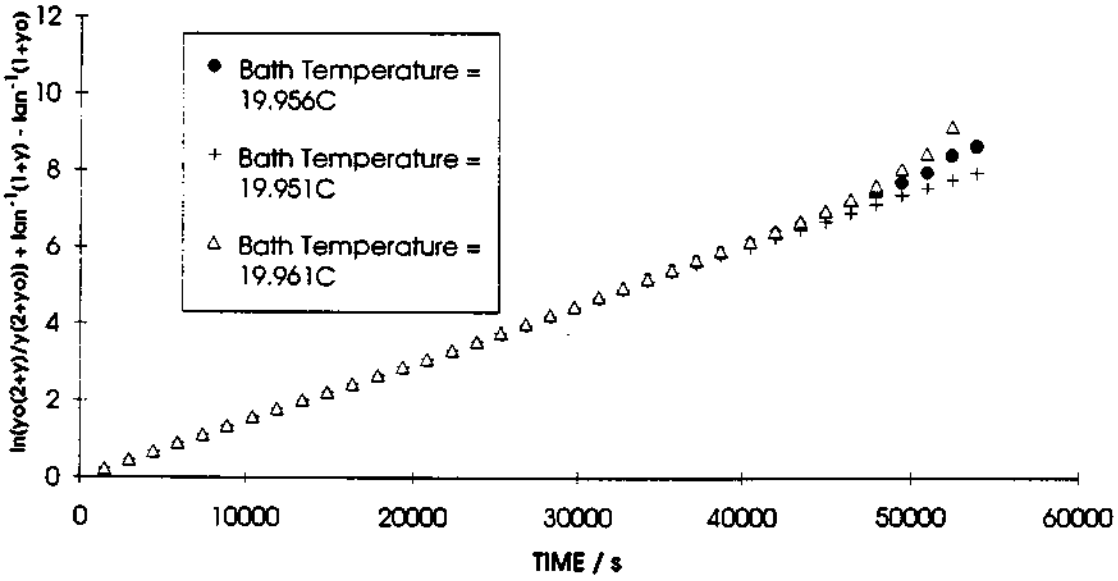

Fig 2. Analysis of a cooling curve according to equation (3) for an electrode following Scenario 2 – $\frac{1}{4}$ mm diameter by 12.5 mm length Pd cathode polarised in 0.1M LiOD in D_2O; final cell current: 200 mA; initial temperature for cooling curve: 51.524°C.

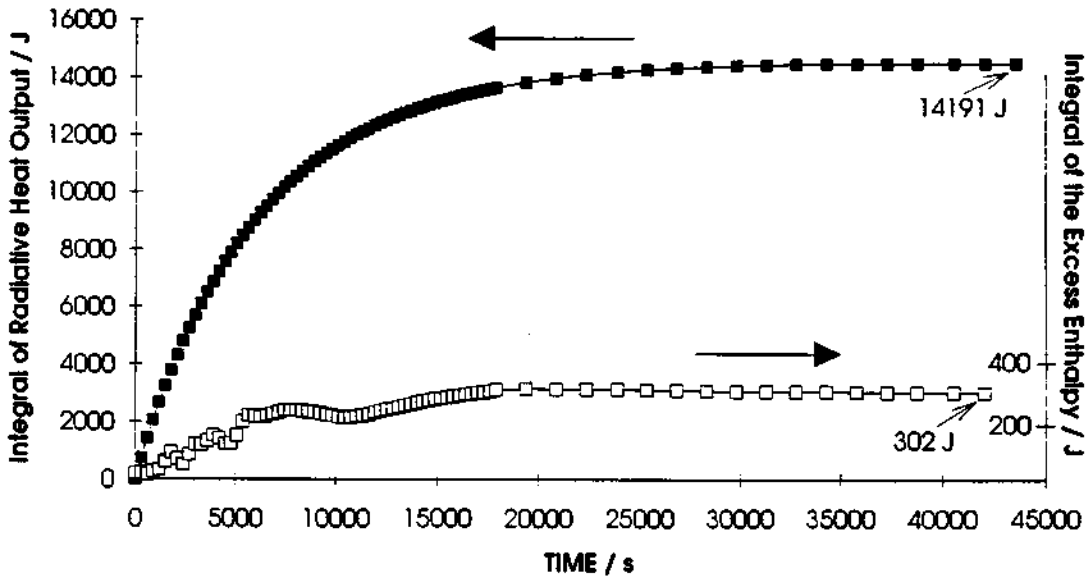

Fig 3. The integral radiative heat output and the integral of the rate of excess enthalpy generation for the example of Fig 2.

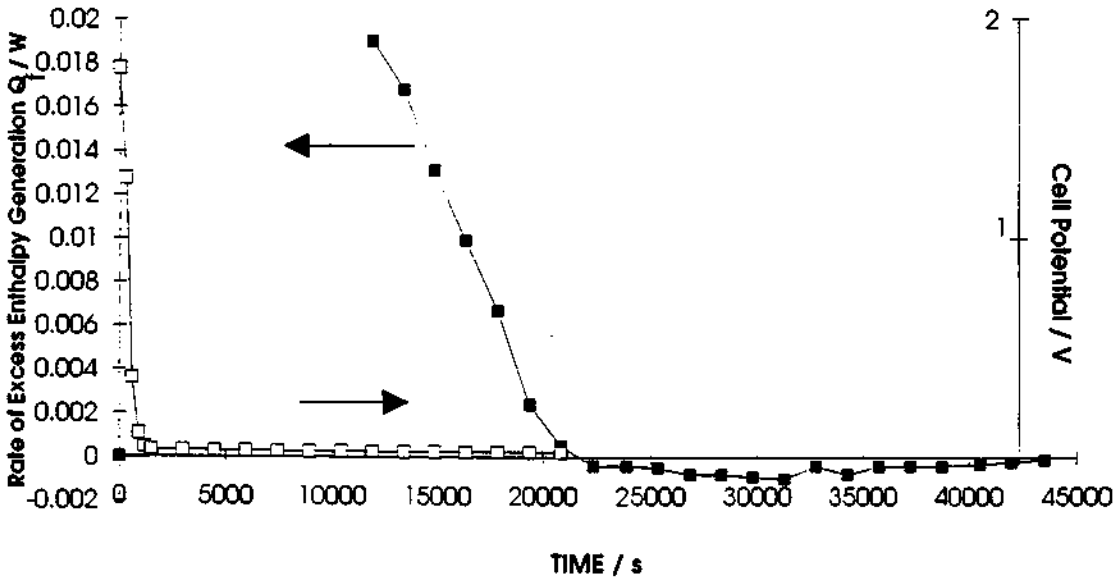

Fig 4. The rate of excess enthalpy generation and the cell potential for the example of Fig 2.

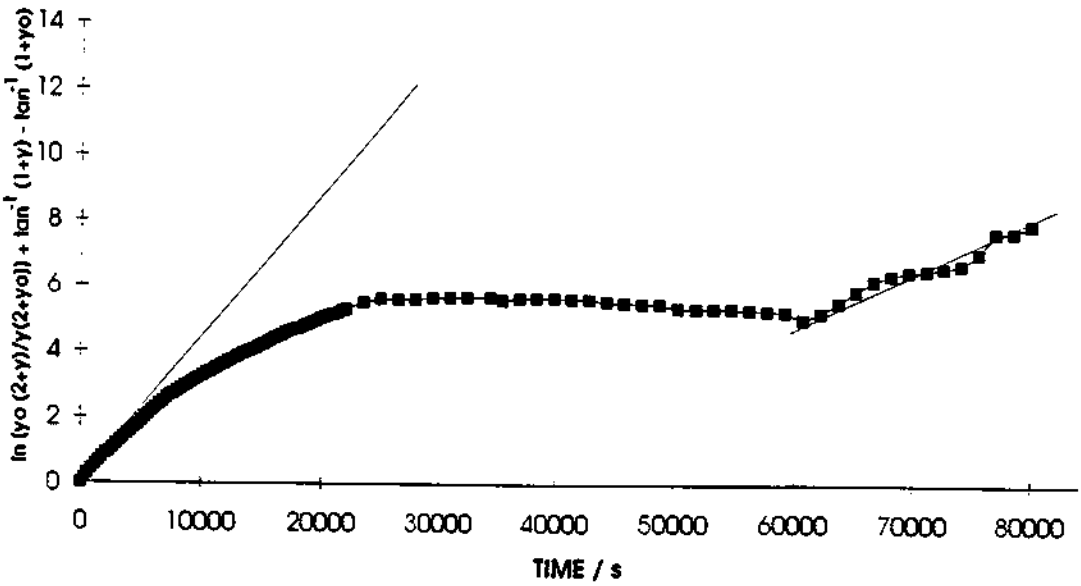

Fig 5. Analysis of a cooling curve according to equation (3) for an electrode following Scenario 4 - 1 mm diameter by 12.5 mm length Pd cathode polarised in 0.1M LiOD in D_2O: final cell current: 250 mA: initial temperature for the cooling curve: 99.605°C.

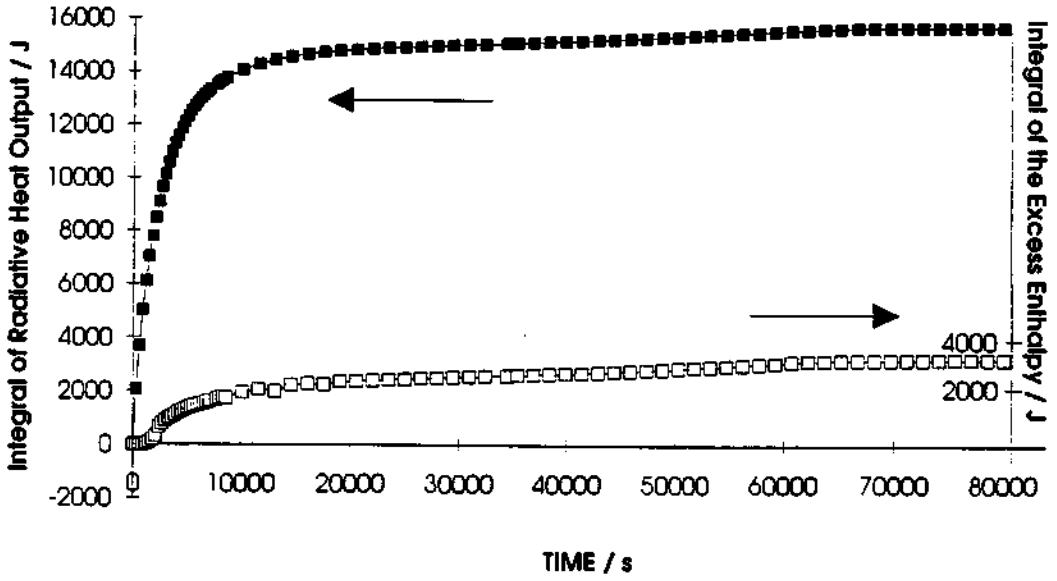

Fig 6. The integral radiative heat output and the integral of the rate of excess enthalpy generation for the example of Fig 5.

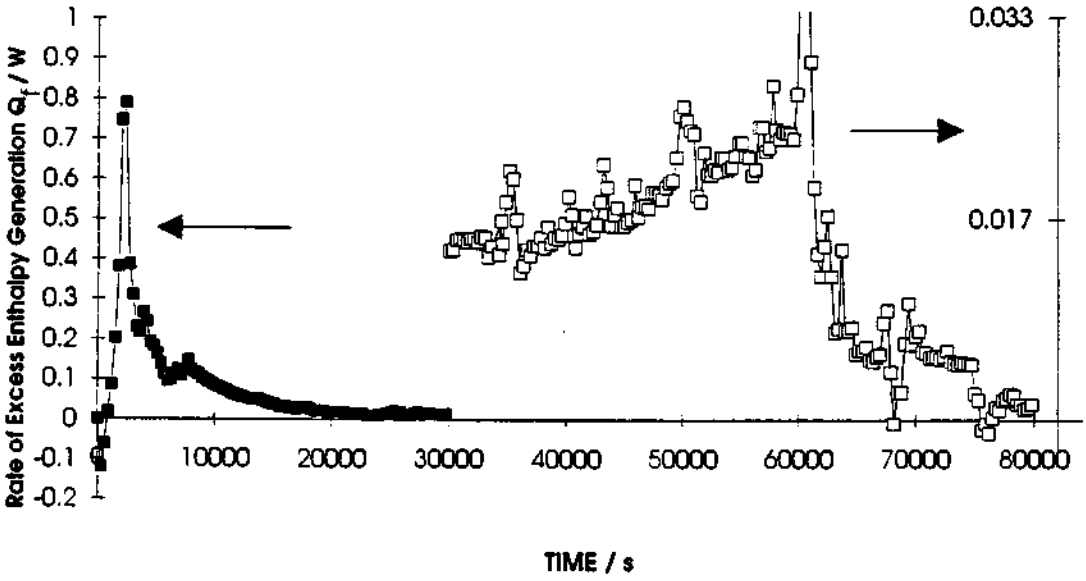

Fig 7. The rate of excess enthalpy generation for the example of Fig 5.

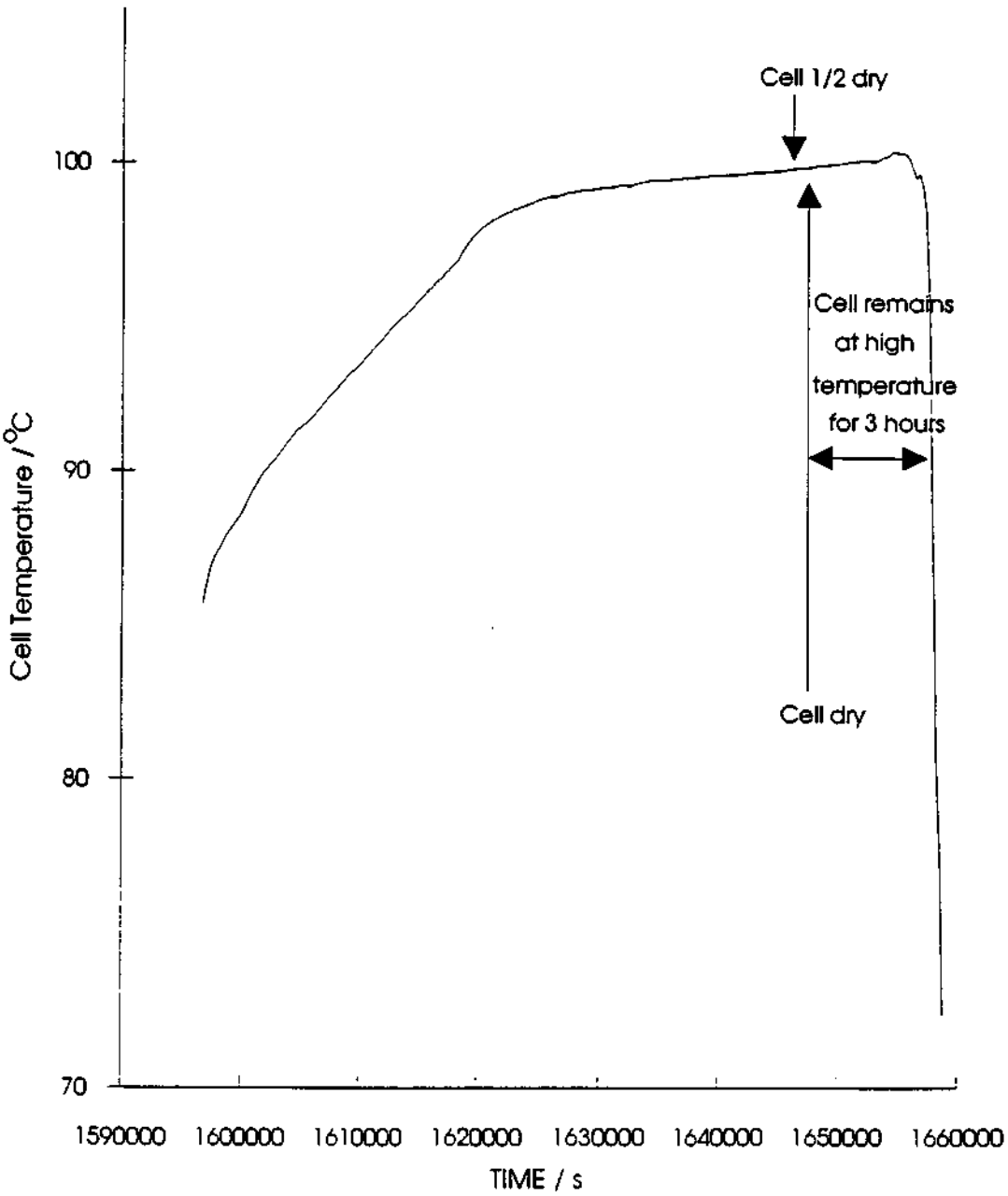

Fig 8. The temperature–time curve for a cell being driven to boiling showing also the initial part of the cooling curve – 2 mm length Pd cathode polarised in 0.1M LiOD in D_2O; final cell current: 500 mA.

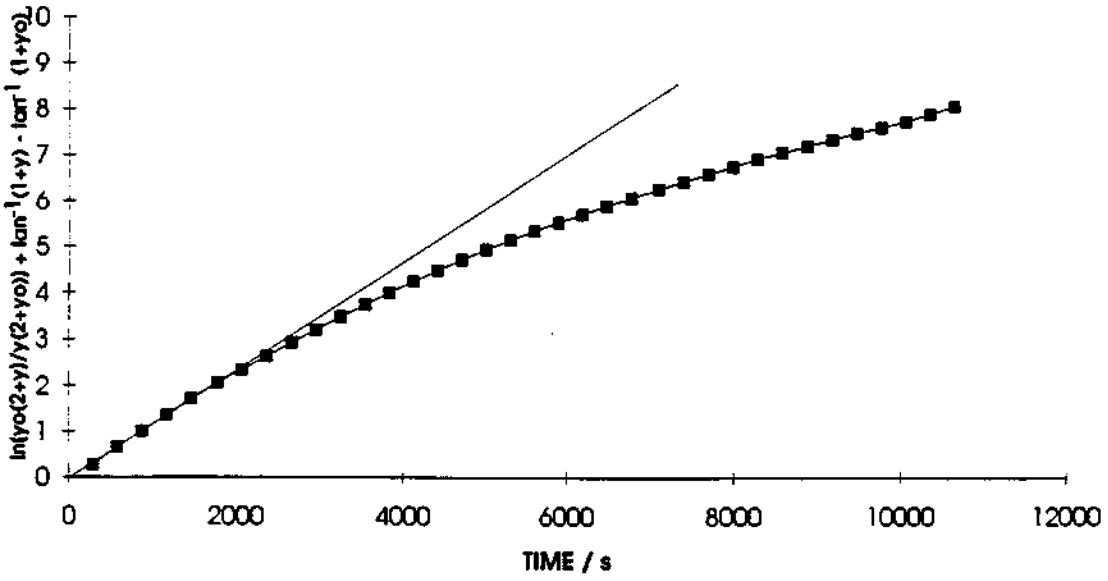

Fig 9. Analysis of the cooling curve for a "blank cell" covering the case of Scenarios 5 and 6.

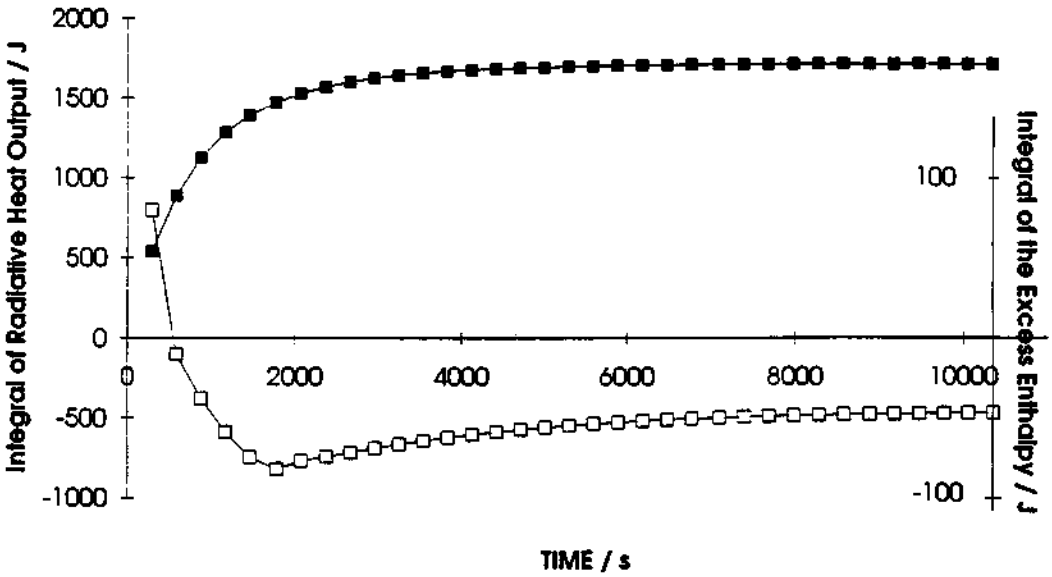

Fig 10. The integral radiative output and the integral of the rate of excess enthalpy generation for the example of Fig 9.

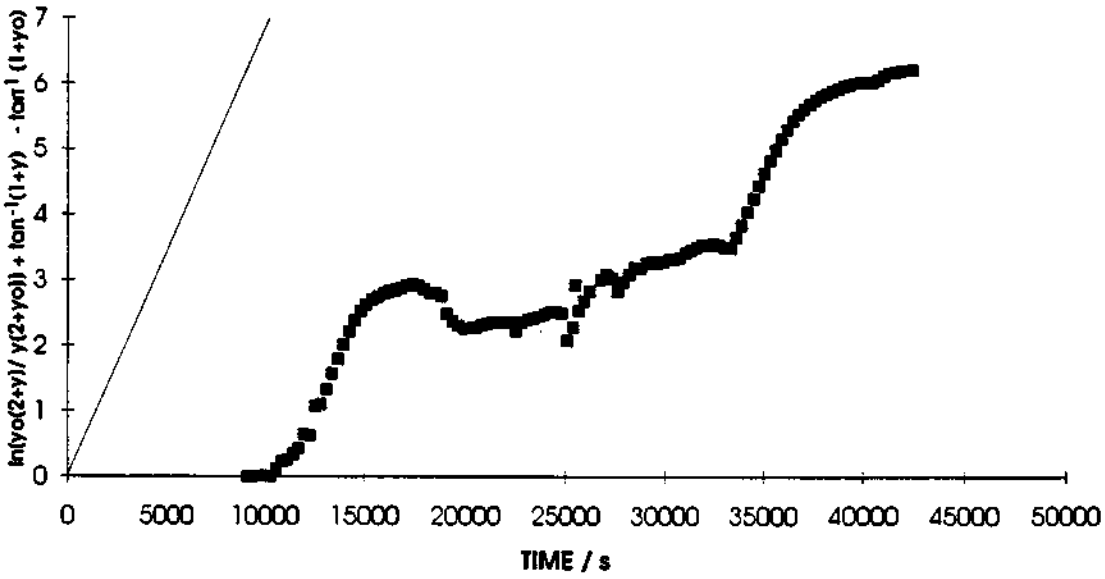

Fig 11. Analysis of the cooling curve according to equation (3) for the example of Fig 8.

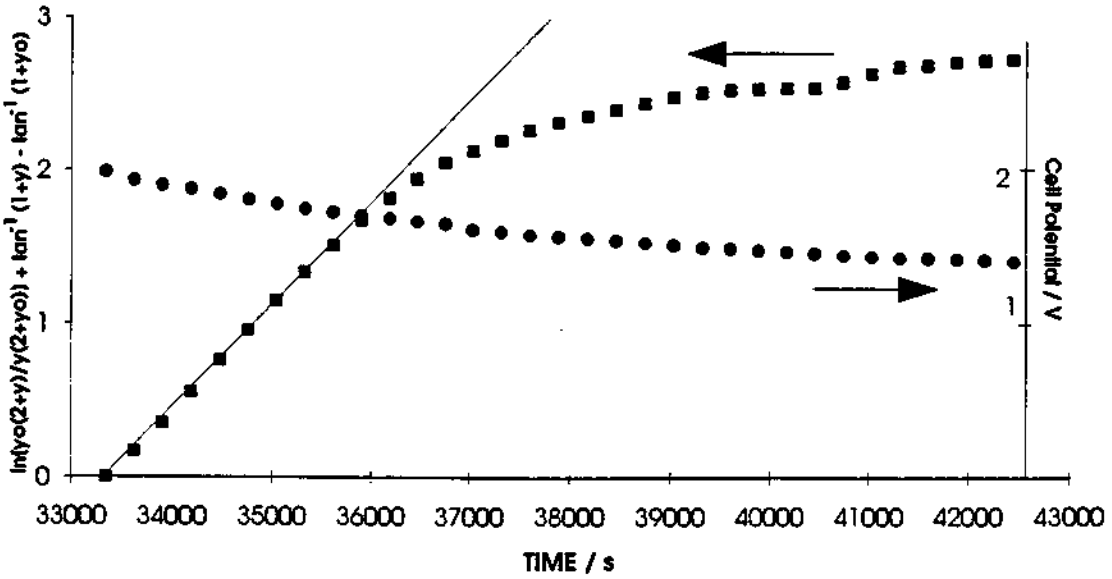

Fig 12. Analysis of the cooling curve according to equation (3) for the example of Fig 8 and at times greater than 33,337 s. The figure also shows the variation of the cell potential with time.

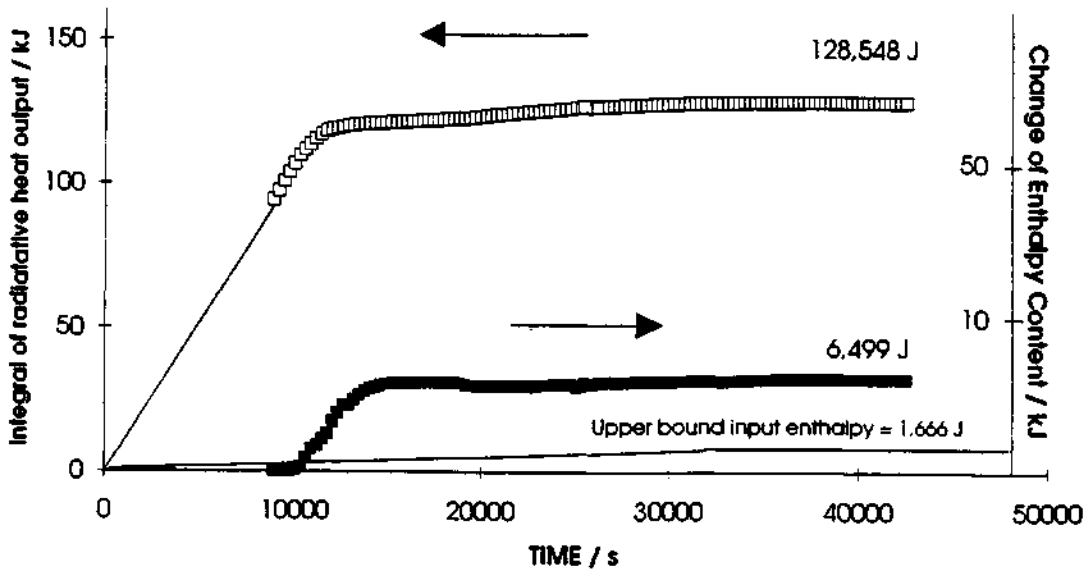

Fig 13. The integral radiative heat output and the change of enthalpy content of the calorimeter for the example of Fig 8.

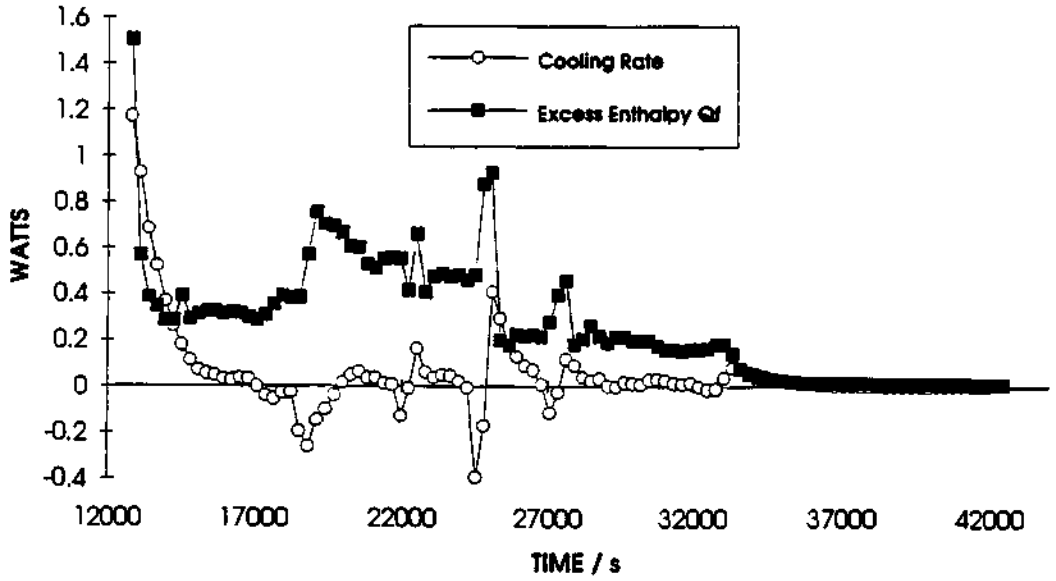

Fig 14. The rate of cooling and the rate of excess enthalpy generation for the example of Fig 8 and at times greater than 12,829 s.